

Analysis of Two Schemes of Cold Forging of a Hollow Ball

Grzegorz Samołyk^{1*}, Grzegorz Winiarski¹

¹ Mechanical Engineering Faculty, Lublin University of Technology, ul. Nadbystrzycka 36, 20-618 Lublin, Poland

* Corresponding author's e-mail: g.samolyk@pollub.pl

ABSTRACT

The paper discusses the cold forging process of a hollow ball made of aluminum alloy. The forging is carried out in dies with a closed cavity, and the billet is shaped like a tube. Two forging schemes are considered. The first scheme is the primary way of forming from a tubular billet, in which the wall deforms freely and is subject to buckling. The second scheme involves the use of an additional tool in the form of a deformable insert consisting of two rings to counteract the uncontrolled deformation of the billet wall. Experimental and theoretical analysis was carried out to compare the progression of forging shape, strain, forging force and stress.

Keywords: cold forging, hollowed balls, deformable insert, strain and stress, FEM.

INTRODUCTION

Products with spherical shapes have applications in almost every sector of the industry. For example, solid balls are commonly used in bearings and mills, hollow balls are used in valves, and other spherical products are components of many mechanisms [1], e.g. they are used in subassemblies of motor vehicles. Balls are made of various materials, with metal products being either cast or shaped by forming methods or even made by machining methods. Narrowing the considerations down to the metal forming methods shows that solid balls are forged [2] or rolled [3, 4]. Hollow balls are also formed by die forging and rolling, but are also successfully shaped by rotary compression [5, 6]. As a rule, these processes are carried out under hot-forming conditions [1], but products of this type can also be warm formed [3] or cold formed [7]. The most significant technological challenge is the shaping of hollow products. Samołyk [2, 7] and Agustin et al. [8] discussed known methods of making hollow balls, in which the inner surface is formed either freely or using a mandrel. Typically, simple mandrels made of non-deformable materials are used [6], which should be removed from the shaped hollow ball.

Flexible mandrels [2] can also be used, which can be made of elastomer or even plastic materials. In such cases, it is recommended to carry out the forming of the hollow ball in cold working conditions. The advantage of using flexible mandrels or inserts is obtaining a concave inner surface of the hollow ball. Graf et al. [9] showed that using the so-called of deformable cores instead of rigid straight mandrels or ever-flexible mandrels may be preferable in many cases of forming process. An aluminum can be used as a deformable core during hot forging of hollow parts, while during cold-forming, low-melting alloys can also be used to make such cores or other inserts [10].

The process of forging hollow balls has several limitations that narrow the ranges of permissible values of final product dimensions. The basic limitation is the buckling of the workpiece wall. The phenomenon of this buckling is discussed, e.g. on the examples of forming cylindrical products [11] and spherical [12]. On the other hand, the types of defects of hollow balls appearing during forging in conditions conducive to wall buckling were also discussed in the work [7] by Samołyk et al. In another work [2], it was shown that a deformable insert is an effective way to counteract this type of limitation in forming spherical products.

Therefore, this paper continues the authors' work on this issue. The aim of the presented research is to compare two methods of forging a hollow ball – without the use of a deformable insert and using a properly profiled insert. The current paper presents only selected results of extensive own research. The shape and proportions of the insert are the result of this research. The scientific purpose of the paper is to explain the phenomenon limiting the forming of the correct forging external outline, to relate this phenomenon to stress and strain, and to explain the effect of using an insert. It also aims to demonstrate the indirect role of using an insert on the change of stress and strain in the material.

CHARACTERISTICS OF THE FORGING PROCESS

The subject of the research is the cold forging process of a hollow ball forging made of aluminum alloy EN AW 6063 (according to PN-EN 573-1:2004). The process is carried out under laboratory conditions using dies of closed design and without the use of additional rigid tools such as mandrels. A ball forging with a diameter of $\varnothing 30$ mm and an average wall thickness of 1.8 mm is formed from a tubular billet with an external diameter of $\varnothing 27$ mm, a height of 29 mm and a wall thickness of 1.8 mm. The top die moves at a constant speed of $v = 1.67$ mm/s until the cavity is completely closed. This scheme of the forging process is shown in Figure 1a.

In the other hand, Figure 1b shows the second variant of the forging process being analyzed. In this variant, a deformable insert is placed inside the tubular billet, consisting of two rings with a diameter of $\varnothing 23.4$ mm, a height of 14 mm and a wall thickness of 4.5 mm. These rings have one-sided bevels, which are shown and dimensioned in Figure 1b. The insert is made of Wood's alloy, i.e. low-melting alloy TBC12, which has a melting point of approximately 98 °C. The choice of this material is due to the following characteristics: good formability, ease of manufacturing (it is an alloy with good castability and zero shrinkage) and ease of removal of the deformed insert from the forged ball (by melting when the insert with forging are heated to a temperature exceeding 100 °C). It should also be noted that the shape and dimensions of these ring bevels are the result of the optimization carried out for the effectiveness of the deformable insert's effect on the ball forging process.

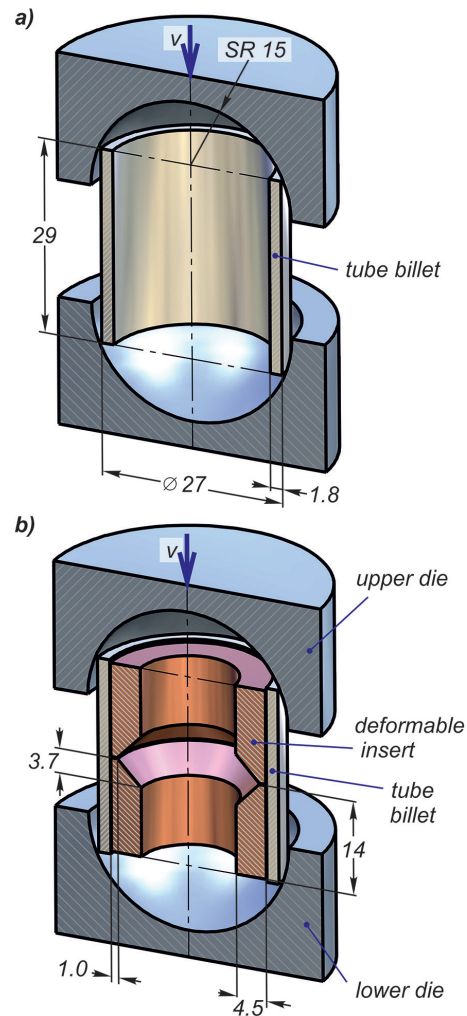


Fig. 1. Schematic of the forging process of a hollow ball with a diameter of $\varnothing 30$ mm using only two dies (a) and using a suitably shaped deformable insert as an additional tool (b)

NUMERICAL CALCULATION OF THE FORGING PROCESS

The numerical analysis was carried out using the Deform-3D software program, which used FEM modelling. The tools were modelled as rigid objects, with the upper die moving at a constant velocity of $v = 1.67$ mm/s, which is in accordance with experimental conditions. The workpiece was modelled as a rigid-plastic object. Geometric symmetry was used in the modelling, i.e. only half of the billet was discretized, as shown in Figure 1. Approximately 100,000 tetragonal elements were used for this discretization. A model representing the EN AW 6063 alloy was used to describe the behavior of the workpiece material, which is in the form of a constitutive equation [2, 7]:

$$\sigma_p = 949(0.0001 + \varphi)^{0.248} \cdot \exp(-0.5209\varphi)\dot{\varphi}^{0.1358} \quad (1)$$

where: σ_p – yield stress;
 φ – effective strain;
 $\dot{\varphi}$ – strain rate.

This model is determined for cold forging conditions at room temperature, where the influence of thermal phenomena is negligible.

For the analysis of the ball forging variant using a deformable insert, the numerical model consisted of three rigid-plastic objects. One object represents the billet while two further objects represent the two inner rings (Figure 1b). Again, geometric symmetry and tetragonal elements were used to discretize the volume of these rings representing the deformable insert. Assuming that the insert material is TBC12 alloy (Bi-Pb25Sn12Cd12), the constitutive Equation 2 was used to describe its behavior under load:

$$\sigma_p = 109.5\varphi^{0.042} \cdot \exp(-0.36\varphi)\dot{\varphi}^{0.16} \cdot \exp(-0.22\dot{\varphi} \cdot 2.6\varphi) \quad (1)$$

where: the same designations as in Equation 1.

It should be mentioned that these equations were obtained in our own research, which was discussed in detail in an earlier paper of our own [2].

The Coulomb friction model was used to describe the contact conditions between deformable objects and rigid tools, assuming a friction coefficient of $\mu = 0.12$. This corresponds to the lubrication conditions found in the experimental tests. On the other hand, between the billet and the deformable insert, the friction coefficient was $\mu = 0.09$. The friction coefficients were determined in a ring upset test between anvils made of the same material as the billet, deformable insert and dies.

Figure 2 and Figure 3 show the simulation results in terms of shape progression and effective strain distribution. In the initial forging phase, a clear compression of the upper and lower edges of the billet is observed. This results in the formation of two holes, the diameter of which decreases with time. At the flank of these holes, the effective strain is greatest. When forging a ball without an insert (Figure 2), low effective strains are observed

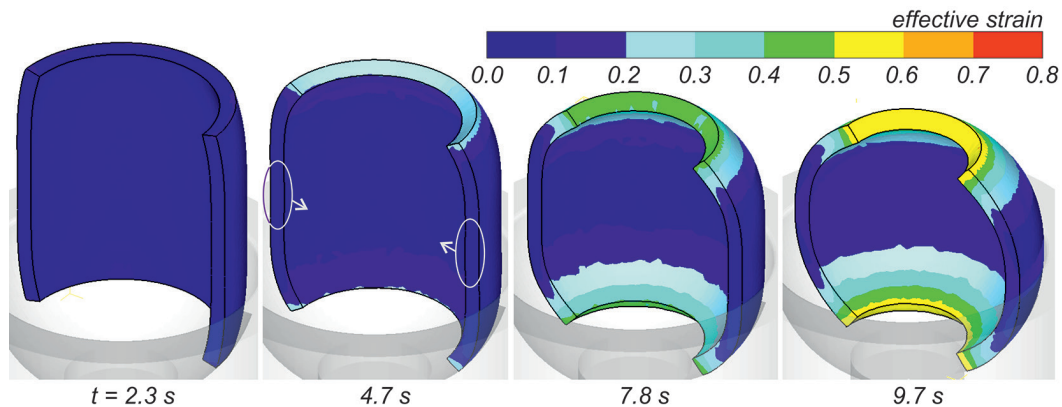


Fig. 2. Shape progression and effective strain distribution during the forging of a hollow ball without a deformable insert – the second figure shows where the concavity of the workpiece wall is being formed

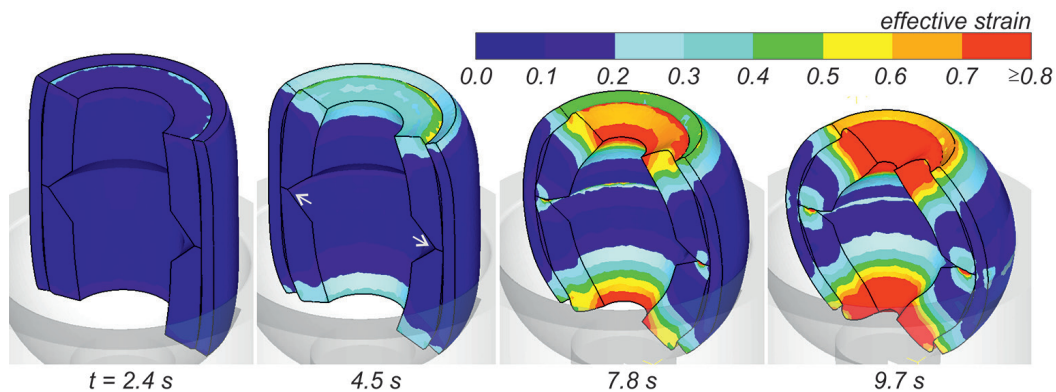


Fig. 3. Shape progression and effective strain distribution during the forging of a hollow ball using a deformable insert (description in the text)

in the central part of the workpiece and there is a tendency for the concave outline of the forging to develop. The result is the inability to obtain a ball with the correct outline. The observed phenomenon is the beginning of buckling of the workpiece walls, which is a process limitation. In contrast, this phenomenon was not observed in the case of forging with the deformable insert, as shown in Figure 3. The flanks of the forming ball holes interact with the rings of the deformable insert in such a way that, in the dies parting plane, the deformable insert counteracts the occurrence of workpiece concave. This has the effect of obtaining a ball with the correct outline and completely eliminating the tendency for the workpiece to buckle. The use of a deformable insert also results in higher effective strains being observed in the workpiece. Simulation has shown that the use of a deformable insert meets the expectations set for it.

EXPERIMENTAL VERIFICATION

Experimental verification was carried out under the conditions of the metal forming laboratory of the Lublin University of Technology on a test stand equipped with an Inston testing machine with a maximum pressure of 1 MN. The tool set shown in Figure 4 was used for the tests. This figure also shows the shape of the billets and inserts, which were made under the same assumptions as in the FEM analysis. The aim of the experimental verification was to validate the numerical model

of the forging process. All boundary conditions assumed during modelling were retained.

First, the shape and dimensions of the resulting forgings were compared with the FEM results. The comparison showed satisfactory qualitative agreement. Quantitatively, the differences between the individual dimensions (i.e. ball diameter, ball hole diameter, forging height) were within 12%. The resulting forgings in the experiment are shown in



Fig. 4. Photograph of the tools used in the experimental verification and the shape of the samples (the billet from which the ball is obtained and the rings from which the deformable insert is created)

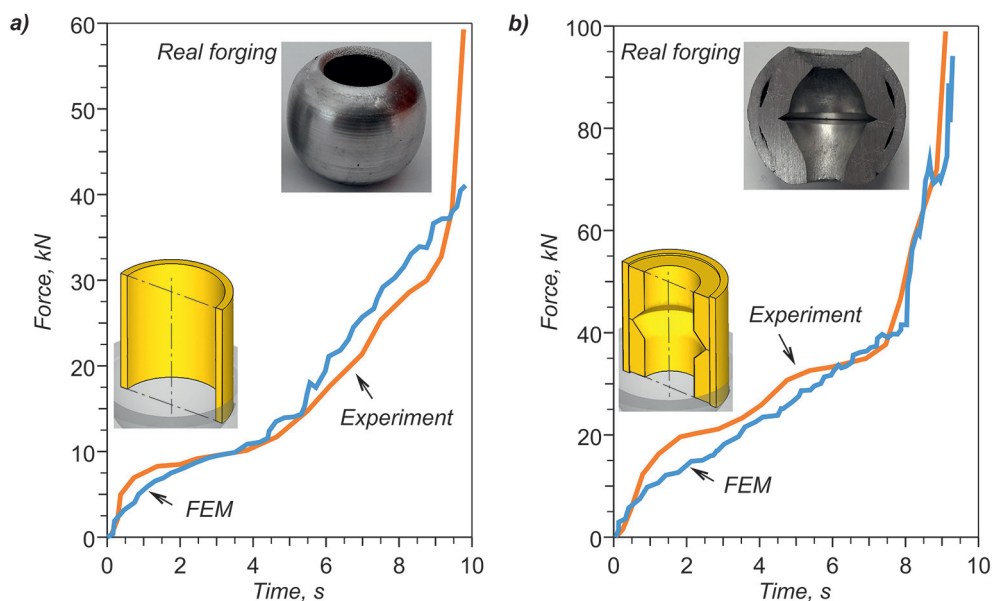


Fig. 5. Shape progression of forged ball forgings without deformable insert (a) and with insert (b) – description in the text

Figure 6. In the case of forging the ball without using a deformable insert (Figure 5a), it was observed that, as in the simulation, the shape of the ball forging strongly deviates from the expected outline. The side surface of the ball is slightly concave. It was also observed that further upsetting does not lead to pronounced buckling and that the final shape of the ball is consistent with that obtained in the numerical calculation (Figure 2). These observations fully confirm the validity of the FEM model. A similar agreement between the calculations and the real results was observed in the case of forming with a deformable insert (Figure 5b). In this case, the formation of an outflow in the plane of the die parting was not observed (as in FEM – Figure 3), despite the fact that the deformable insert clearly pushes the side wall of the workpiece outside the die cavity. The closing of the dies counteracts the creation of flash.

Force parameters were also compared. A comparison of the forming force is shown in Figure 6. Initially, the measured force is slightly higher than the calculated force. In the case of ball forming without deformable insert, there is a time when this force is even lower. Towards the end of the forging process, the real force increases sharply, which is related to the closing of the dies. Nevertheless, the real force oscillates within the calculated force, keeping the same tendency. This observation allows us to conclude that qualitative and quantitative agreement is maintained. The observed differences are due to the fact that during FEM modelling, the friction conditions are fixed (a constant friction coefficient value was

assumed). In reality, the coefficient of friction is not constant, which is confirmed by visual inspection of the working surfaces of the tool's cavity (Figure 4), which show traces of wear (after dozens of forging tests). Figure 6b also shows a photograph of a cross-section of an real ball forging obtained under experimental conditions.

COMPARISON OF TWO SCHEMES OF HOLLOW BALL FORGING PROCESS

The main problem of forging process of a hollow ball without the use of a deformable insert is the difficulty of maintaining the expected wall outline. The solution to this problem is to use an insert to interact with the wall of the workpiece from the inside. In order to compare the two forging schemes, 30 tracking points were placed on the side wall of the billet at an equal distance of 1 mm (Figure 7), which are sensors that track the selected parameters. Point no. 1 is located at the edge of the billet in contact with the bottom die at the start of the forging process, while point no. 30 is in contact with the upper die. Points 15 and 16 are located within the parting plane of the die (approximately halfway up the billet).

Figure 8 shows a comparison of the change in the external outline of the workpiece wall (in $\{r, z\}$ coordinates – i.e. radial and axial) during forging without the insert (line A) and with the deformable insert (line B). This outline in the form of a line graph is summarized for six selected times t of the forging process. On the other



Fig. 6. Comparison of the forming force calculated in FEM and measured experimentally during the ball forging without deformable insert (a) and with insert (b)

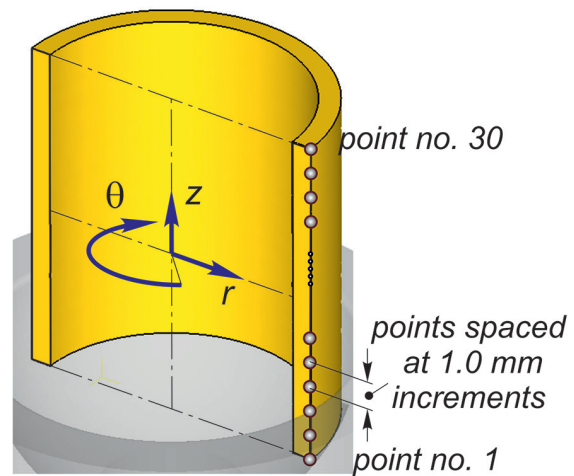


Fig. 7. Arrangement of the 30 tracking points (sensors) on the lateral surface of the billet and the cylindrical coordinate system $\{r, z, \theta\}$ taken at mid-height of the billet

hand, an additional bar graph shows the Δr increments for the selected sensors for specific time intervals of the forging process, equal to 1.5 s, i.e. the graph in Figure 8a represents Δr increments from 0 to 1.5 s, the graph in Figure 8b from 1.5 s to 3.0 s, etc., up to Figure 8f, which represents Δr increments from 7.5 s to 9.0 s. In addition, the maximum difference of these increments between the two forging schemes A and B, i.e. the values labelled Δ_{AB} , are included in these graphs.

It can be seen from Figure 8 that the deformable insert fulfils its role from the very beginning of the forging process (scheme B). At the start of the process, the insert not only prevents the formation of a concave wall outline, but also causes a slight outward pushing of the workpiece wall in the direction of the radius r . This phenomenon becomes more

intensive with time, and the strongest effect of the insert is observed in the time interval t between 6 s and 7.5 s. Considering the results shown in Figure 3, it is concluded that the main reason for obtaining such a favorable effect of the deformable insert on the workpiece wall is the execution of appropriate undercutting of the rings at the height of the dies parting plane. The line B shown in Figure 8f is also the preferred final outline of the ball forging.

The next Figure 9 shows the distribution of the three components of stress measured in the sensors for three selected moments of the ball forging process, which is a variant without the use of an insert. Special attention should be focused on the points located in the vicinity of the dies parting plane, i.e. points 11 to 20. This group of points belongs to the lateral surface of the workpiece, which, according to

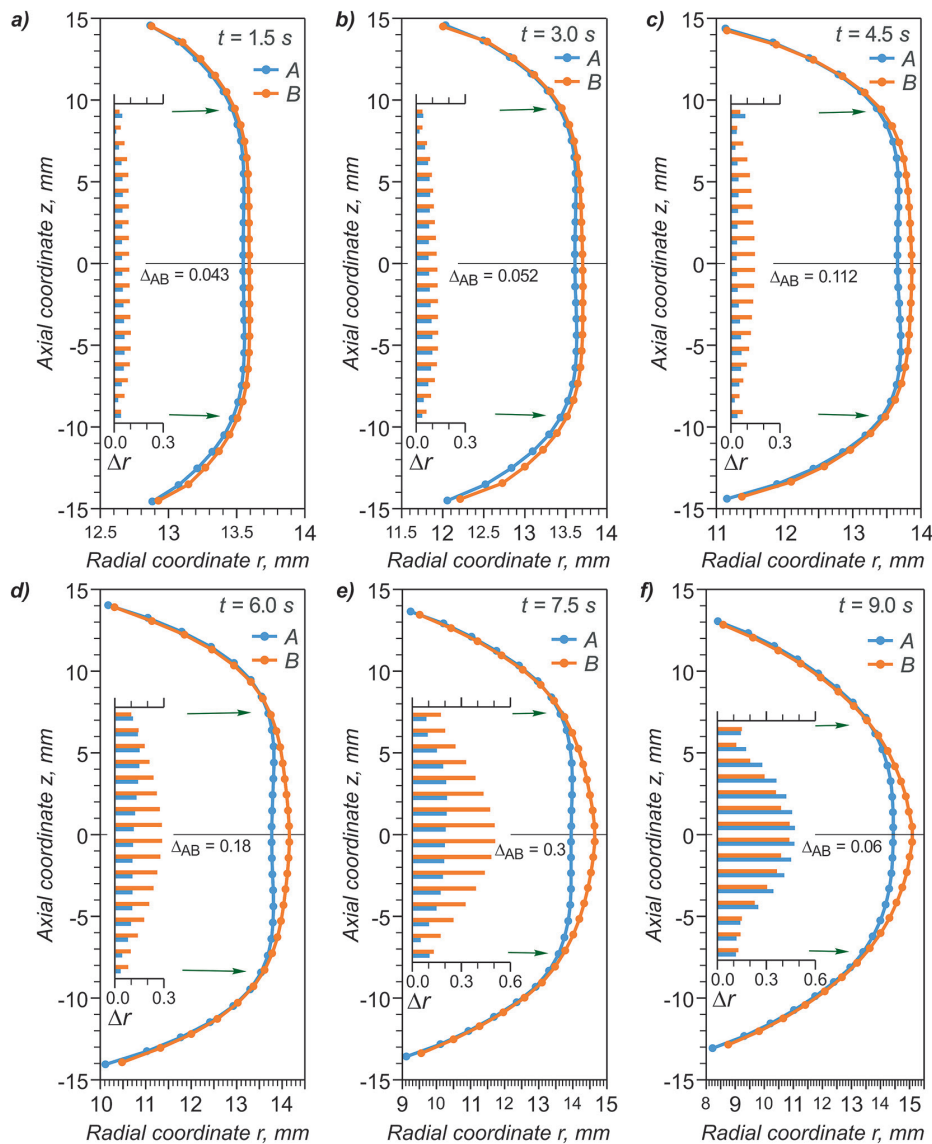


Fig. 8. Comparison of the change in sensor coordinates representing the external outline of a forged ball wall without (line A) and with (line B) a deformable insert – full description in the text

Figure 8, is not concave at the selected process time. The radial stress σ_r has basically a neutral effect on the observed phenomenon of the formation of the workpiece's side wall, since its value is close to zero. The circumferential stress σ_θ has positive values, causing tension in this direction, but its values are relatively small. The largest absolute values are reached by the axial stress σ_z , especially at points 15 and 16. This stress is compressive in nature. In summary, the reason for obtaining a non-convex lateral surface of the ball forging is the state of stress in

the form of a slight tensile circumferential stress and a significant compressive axial stress. The use of a deformable insert causes a change in the stress pattern around the center points numbered 15 and 16. According to Figure 10, the role of the axial component of the stress is minimized to that of the radial component, while the circumferential component of the stress σ_θ begins to play a significant role. This stress component still has a tensile character, but its absolute value is significantly higher than the previously mentioned cases (Fig. 10b).

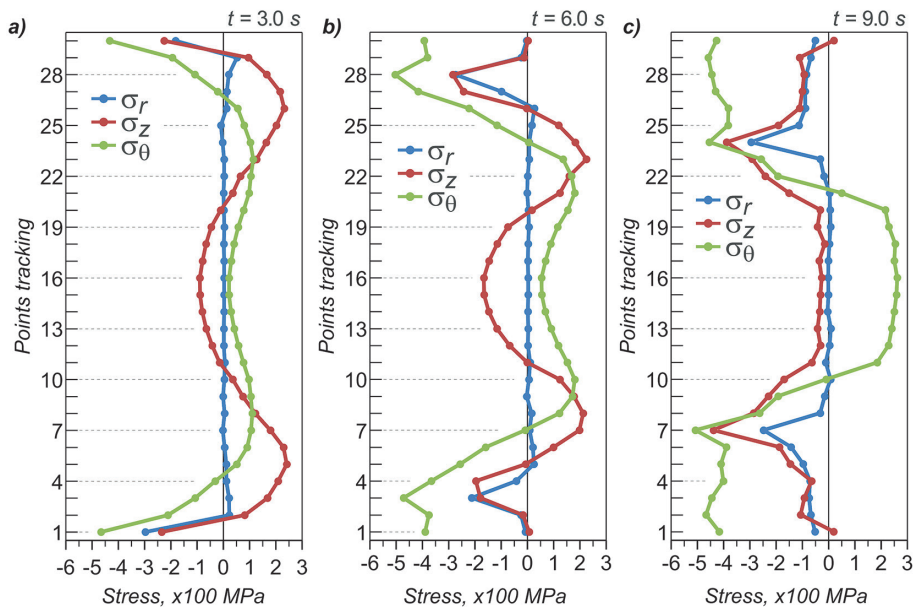


Fig. 9. Distribution of stress components in the sensors (according to Figure 7) for three selected moments of the hollow ball forging process without the use of a deformable insert

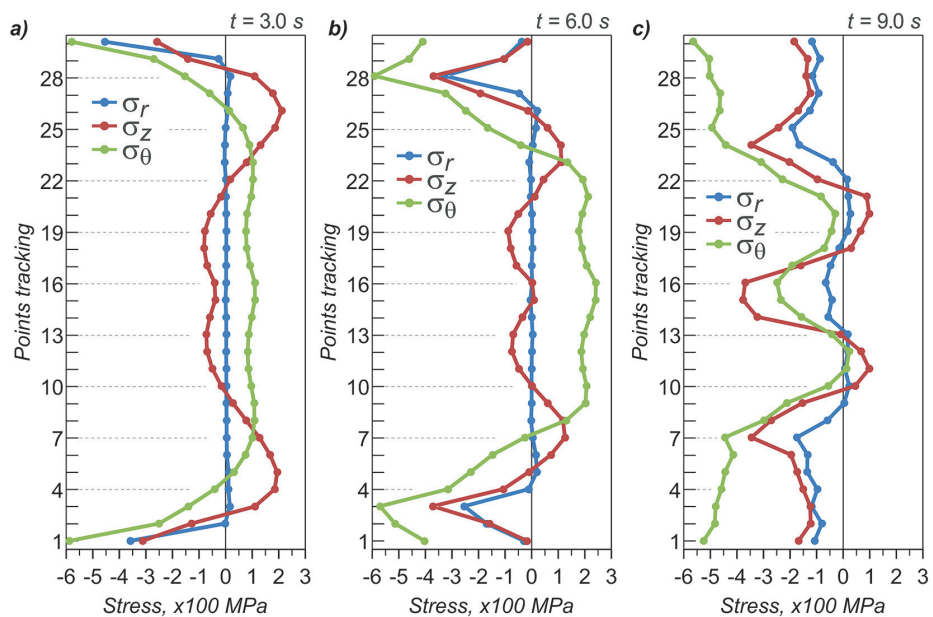


Fig. 10. Distribution of stress components in the sensors (according to Figure 7) for three selected moments of the hollow sphere forging process using a deformable insert

The arrangement of stress components shown in Figure 9c is similar to that in Figure 10b for points 15 and 16. This means that such an arrangement of stress components favors the formation of a convex side surface of the shaped hollow ball. Thus, it should dominate throughout the process at those points of the wall that are in the vicinity of the dies parting plane. The study shows that the use of a deformable insert consisting of two properly chamfered rings makes it possible to achieve the expected stress state in the formed workpiece wall. On the other hand, the system of stress components observed at the end of the forging process with the deformable insert (Fig. 10c – points 15 and 16) is a system typical of the phenomenon of the so-called inhibition of the enlargement of the hollow ball diameter. In this case, it is caused by the closing of the dies at the final stage of the forging process.

CONCLUSIONS

A comparison of two cold forging schemes for a hollow ball showed that the use of an additional deformable tool in the form of a deformable insert makes it possible to obtain a forging with the expected correct shape. The effect of this insert on the inner wall of the shaped ball was shown to be beneficial. It eliminates shape defects and prevents the formation of a non-convex surface of the ball forging around the dies parting plane. The favorable effect of this insert also causes a change in the state of stress registered on the outer surface of the workpiece. The results also make it possible to identify this stress state and explain its influence on the way the outline of the forging is formed. Unfortunately, the use of a deformable insert causes an increase in the forming force, at least twice. Based on the results presented, the following final conclusions can be drawn. In order for the deformable insert to fulfill its purpose, it must have the right shape and dimensions in relation to the dimensions of the charge, with the key feature of this shape being the implementation of special undercuts (chamfers) at the height of the dies parting plane. In order to obtain a convex outer wall surface in the formed forging, the deformable insert must induce a favorable state of stress in this wall at the height of the dies parting plane, i.e., the circumferential stress component must have a tensile character with a value as large as possible, the absolute value of the axial component (which is inherently compressive) should be as close to zero as possible, while the radial component (which is inherently close to zero) does not play an important role in this problem.

Acknowledgments

The research was financed from the funds of the Scientific Discipline Council for Mechanical Engineering: M/KOPM/FD-20/IM-5/101/2022.

REFERENCES

1. Bulzak T., Tomczak J., Pater Z., Majerski K. A Comparative Study of Helical and Cross-Wedge Rolling Processes for Producing Ball Studs. *Materials* 2019; 12(18): 1–11.
2. Samołyk G., Winiarski G., Gontarz A. A cold forging process for producing thin-walled hollow balls from tube using a plastic insert. *International Journal of Advanced Manufacturing Technology* 2020; 108: 1429–1446.
3. Bulzak T., Majerski K., Tomczak J., Pater Z., Wójcik Ł. Warm skew rolling of bearing steel balls using multiple impression tools. *CIRP Journal of Manufacturing Science and Technology* 2022; 38: 288–298.
4. Wójcik Ł., Pater Z., Bulzak T., Tomczak J., Lis K. A Comparative Analysis of the Physical Modelling of Two Methods of Balls Separation. *Materials* 2021; 14(23): 1–20.
5. Skrochocki D., Tomczak J. Numerical simulation of rotary compression process of hollow balls. *Strength of Materials* 2016; 48(4): 583–591.
6. Tomczak J., Pater Z., Bulzak T. A theoretical and experimental analysis of rotary compression of hollow forging formed over a mandrel. *Strength of Materials* 2017; 49(4): 555–564.
7. Samołyk G., Winiarski G. Selected aspects of a cold forging process for hollow balls. *International Journal of Advanced Manufacturing Technology* 2022; 119 (3–4): 2479–2494.
8. Augustin C., Hungerbach W. History and Production of Hollow Spheres. *Multifunctional Metallic Hollow Sphere Structure* 2009; EM: 5–30.
9. Graf M., Härtel S., Binotsch C., Awiszus B. Forging of lightweight hybrid metallic-plastic components. *Procedia Engineering* 2017; 184: 497–505.
10. Wang L., Li M., Zhao L., Guo Y. Research on a wrinkle-free forming method using low-melting alloy for sheet metal. *International Journal of Advanced Manufacturing Technology* 2018; 99(9–12): 3065–3075.
11. Alhussainy F., Sheikh M., Hadi M. Behaviour of small diameter steel tubes under axial compression. *Structures* 2017; 11: 155–163.
12. Rots J.G., Hoogenboom P.C., van der Meer F.P., Borgart I. Local Buckling Analysis of Thin-Wall Shell Structures. Master Thesis Project 2015; Delft University of Technology: 1–137.